Available online at www.sciencedirect.com
ScienceDirect
Journal of Computational and Applied Mathematics 200 (2007) 231 – 254
JOURNAL OF COMPUTATIONAL AND APPLIED MATHEMATICS
www.elsevier.com/locate/cam

Error analysis of the Trefftz method for solving Laplace's eigenvalue problems

Zi-Cai Li[a, b, c]

[a]Department of Applied Mathematics, National Sun Yat-Sen University, Kaohsiung, Taiwan 80424, Taiwan
[b]Department of Computer Science and Engineering, National Sun Yat-Sen University, Kaohsiung, Taiwan 80424, Taiwan
[c]National Center for Theoretical Sciences, Taiwan

Received 18 June 2005; received in revised form 19 December 2005

Abstract

For solving Laplace's eigenvalue problems we propose new algorithms using the Trefftz method (TM) (i.e., the boundary approximation method (BAM)), by means of degeneracy of numerical Helmholtz equations. Since piecewise particular solutions can be fully adopted, the new algorithms benefit high accuracy of eigenvalues and eigenfunctions, low cost in CPU time and computer storage. Also the algorithms can be applied to solve the problems with multiple interfaces and singularities. In this paper, error estimates are derived for the approximate eigenvalues and eigenfunctions obtained. Numerical experiments for smooth and singular solutions are reported in this paper to show significance of the algorithms proposed and to verify the theoretical results made.

MSC: 65N30

Keywords: Trefftz method; Boundary approximation method; Eigenvalue problem; Helmholtz equation; Interfaces

1. Introduction

For solving eigenvalue problems, there exist a number of numerical methods, see [5,9,11,19,21,3,24,20,8]. The techniques using particular solutions are given in [4,7,8,18,23]. In this paper we shall follow the ideas in [8] but adopt *piecewise* particular solutions as in [17], by the help of an iteration algorithm. We will solve an auxiliary Helmholtz equation with a non-homogeneous boundary condition and choose a parameter k^2 to approach an eigenvalue. In this method, the solution domain is divided into several subdomains, and different particular solutions on subdomains (i.e., piecewise particular solutions) of the Helmholtz equations are employed to be admissible functions. An approximation of the Helmholtz solutions is then obtained by satisfying only the interior and exterior boundary conditions of the Helmholtz equation. Then approximate eigenvalues and eigenfunctions can be found by an iteration method, in which the values of k^2 are modified to approach the target eigenvalue. Obviously, using piecewise particular solutions is well suited for solving the eigenvalue problems with multiple interfaces and singularities. Moreover, the approximate solutions may reach high accuracy by a modest effort in computation.

E-mail address: zcli@math.nsysu.edu.tw.

0377-0427/$ - see front matter
doi:10.1016/j.cam.2005.12.017

Although the new algorithms for eigenvalue problems are presented in [14], no error analysis has been provided so far. This paper is devoted to estimate error bounds of the eigenvalues and the eigenfunctions obtained. The paper is organized as follows. In the next section, the algorithms are described. An error analysis is made for eigenvalues and eigenfunctions in Sections 3 and 4, respectively. In the last two sections, numerical experiments of smooth and singular solutions are reported to support the algorithms proposed, and to confirm the theoretical analysis made.

2. Numerical algorithms

Consider the eigenvalue problem

$$\begin{cases} -\Delta\phi_l = \lambda_l \phi_l & \text{in } \Omega, \\ \phi_l|_\Gamma = 0, \end{cases} \tag{2.1}$$

where $\Delta = \partial^2/\partial x^2 + \partial^2/\partial y^2$, and Ω is a polygonal domain with the external boundary Γ. Denote the eigenvalues λ_l in an ascending order

$$0 < \lambda_1 \leqslant \lambda_2 \leqslant \cdots \leqslant \lambda_l \leqslant \cdots . \tag{2.2}$$

The eigenfunctions ϕ_l will satisfy the orthogonality property:

$$(\phi_i, \phi_j) = \int\int_\Omega \phi_i \phi_j \, \mathrm{d}\Omega = \delta_{ij} = \begin{cases} 1 & i = j, \\ 0 & i \neq j. \end{cases} \tag{2.3}$$

Let the solution domain Ω be divided into subdomains, Ω^+ and Ω^- by a piecewise straight Γ_0. Then the eigenfunctions ϕ_l must satisfy the following equations:

$$\begin{cases} -\Delta\phi_l = \lambda_l \phi_l & \text{in } \Omega^+ \text{ and } \Omega^-, \\ \phi_l^+ = \phi_l^-, \ \dfrac{\partial \phi_l^+}{\partial \nu} = \dfrac{\partial \phi_l^-}{\partial \nu} & \text{on } \Gamma_0, \\ \phi_l|_\Gamma = 0, \end{cases} \tag{2.4}$$

where ν is the unit normal to Γ_0. Define an auxiliary Helmholtz solution u to satisfy the following equation:

$$\begin{cases} -\Delta u = k^2 u & \text{in } \Omega^+ \text{ and } \Omega^-, \\ u^+ = u^-, \quad \dfrac{\partial u^+}{\partial \nu} = \dfrac{\partial u^-}{\partial \nu} & \text{on } \Gamma_0, \\ u|_\Gamma = g, \end{cases} \tag{2.5}$$

where $k > 0$, g is a positive function given such that $g \in H^{1/2}(\Gamma)$, and $g \in H^{1/2}(\Gamma)$ is the Sobolev space with semi-norms. Also define the smallest, relative distance between k^2 and λ_i,

$$\delta = \min_i \left| \frac{k^2 - \lambda_i}{k^2} \right| . \tag{2.6}$$

Since $\delta > 0$ in general, the solution u of (2.5) can be obtained by the Trefftz method (TM) (i.e., the boundary approximation method (BAM)), see [22,12,15–17]. Hence we may choose k^2 so as to approach an eigenvalue needed, and then u also approaches its corresponding eigenfunction (see [8]). Let us describe the algorithms in detail below.

2.1. The Trefftz methods

Define a space

$$H = \{v \in L_2(\Omega) | v \in H^1(\Omega^+), v \in H^1(\Omega^-) \text{ and } \Delta v + k^2 v = 0 \text{ in } \Omega^+ \text{ and } \Omega^-\}, \tag{2.7}$$

and a functional

$$I(v)=\int_{\Gamma}(v-g)^2\,\mathrm{d}s+\int_{\Gamma_0}(v^+-v^-)^2\,\mathrm{d}s+\sigma^2\int_{\Gamma_0}(v_\nu^+-v_\nu^-)^2\,\mathrm{d}s, \tag{2.8}$$

where $H^1(\Omega^+)$ and $H^1(\Omega^-)$ are the Sobolev spaces, and σ is a positive weight. We shall use a bilinear form $[u,v]$ on $H\times H$ defined by

$$[u,v]=\int_{\Gamma}uv\,\mathrm{d}s+\int_{\Gamma_0}(u^+-u^-)(v^+-v^-)\,\mathrm{d}s+\sigma^2\int_{\Gamma_0}(u_\nu^+-u_\nu^-)(v_\nu^+-v_\nu^-)\,\mathrm{d}s, \tag{2.9}$$

and the induced norm on the boundary Γ and Γ_0 is defined by

$$|v|_B=[v,v]^{1/2}=\{|v|^2_{\Gamma}+|v^+-v^-|^2_{\Gamma_0}+\sigma^2|v_\nu^+-v_\nu^-|^2_{\Gamma_0}\}^{1/2}. \tag{2.10}$$

The norms $\|v\|_H$ and $|v|_H$ over H are also defined by

$$\|v\|_H=\{\|v\|^2_{1,\Omega^+}+\|v\|^2_{1,\Omega^-}\}^{1/2},\quad |v|_H=\{|v|^2_{1,\Omega^+}+|v|^2_{1,\Omega^-}\}^{1/2}, \tag{2.11}$$

where $\|v\|^2_{1,\Omega^+}$ and $|v|^2_{1,\Omega^+}$ are the Sobolev norms. Also define the finite-dimensional space $S_{m,n}\subseteq H$ such that

$$S_{m,n}=\left\{v|v=v^+=\sum_{i=1}^{m}c_i\Psi_i^+\ \text{in}\ \Omega^+,\ \text{ and }\ v=v^-=\sum_{i=1}^{n}d_i\Psi_i^-\ \text{in}\ \Omega^-\right\}, \tag{2.12}$$

where $\{\Psi_i^{\pm}\}$ are the complete particular solutions of (2.5) in $\Omega^{\pm}$, and c_i and d_i are the coefficients.

When $\delta>0$, a boundary approximation $u_{m,n}\in S_{m,n}$ to problem (2.5) can then be found by the TM:

$$I(u_{m,n})=\min_{v\in S_{m,n}} I(v), \tag{2.13}$$

which leads to a system of linear algebraic equations

$$\mathbf{Ax}=\mathbf{b}, \tag{2.14}$$

where $\mathbf{x}$ is the unknown vector consisting of all expansion coefficients c_i and d_i in (2.12). This TM can also be presented in a weak form

$$[u_{m,n},v]=\int_{\Gamma}gv\,\mathrm{d}s,\quad \forall v\in S_{m,n}, \tag{2.15}$$

and the stiffness matrix $\mathbf{A}$ is non-negative definite and symmetric, given in

$$[u_{m,n},u_{m,n}]=\tfrac{1}{2}\,\mathbf{x}^{\mathrm{T}}_{\mathbf{m,n}}\mathbf{A}\mathbf{x}_{\mathbf{m,n}}. \tag{2.16}$$

The Helmholtz solution should be scaled by dividing the leading coefficient c_1 in (2.12) (see [14]), i.e.,

$$\overline{u}_{m,n}=u_{m,n}/c_1,\quad \overline{\mathbf{x}}_{\mathbf{m,n}}=\mathbf{x}_{\mathbf{m,n}}/c_1,\ \ c_1\neq 0. \tag{2.17}$$

Since $u_{m,n}$ in (2.15) is essentially a least squares solution of (2.13), we will employ the QR method or the singular value decomposition of Golub and van Loan [9] and Atkinson [2], to reduce the condition number, given by

$$\text{Cond.}=\text{Cond.}(\mathbf{A})=\left[\frac{\lambda_{\max}(\mathbf{A})}{\lambda_{\min}(\mathbf{A})}\right]^{1/2}, \tag{2.18}$$

where $\lambda_{\max}(\mathbf{A})$ and $\lambda_{\min}(\mathbf{A})$ are the maximal and the minimal eigenvalues of $\mathbf{A}$, respectively.

2.2. Iterative algorithms for seeking eigenvalues and eigenfunctions

For seeking both eigenvalues and eigenfunctions, we give an iterative algorithm by the following five steps, to modify k for minimizing $\lambda_{\min}(\mathbf{A}(k))$.

Step 1. To approximate a target eigenvalue λ_l, choose suitable term numbers m and n, and three good initial values

$$k_i \approx \sqrt{\lambda_l}, \quad i = 0, 1, 2. \tag{2.19}$$

Step 2. Form the admissible functions $u_{m,n}$ for k_i from (2.12), obtain the scaled solution $\bar{u}_{m,n}$ by the TM in Section 2.1, and evaluate the minimal eigenvalue

$$f(k_i) = \lambda_{\min}(\mathbf{A}(k_i)) = d_{\min}^2. \tag{2.20}$$

Step 3. A quadratic function $P_2(k)$ to approximate $f(k)$ can be formulated by interpolation through three pairs: $(k_i, f(k_i))$, $i = n, n-1, n-2$, where k_i are distinct. A new value k_{n+1} can be found by $P_2'(k_{n+1}) = 0$, to get

$$k_{n+1} = \frac{k_n + k_{n-1}}{2} - \frac{1}{2}\frac{f[k_n, k_{n-1}]}{f[k_n, k_{n-1}, k_{n-2}]}, \quad n \geqslant 2, \tag{2.21}$$

where the divided differences are given by (see [2])

$$f[k_n, k_{n-1}] = (f(k_n) - f(k_{n-1}))/(k_n - k_{n-1}), \tag{2.22}$$

$$f[k_n, k_{n-1}, k_{n-2}] = (f[k_n, k_{n-1}] - f[k_{n-1}, k_{n-2}])/(k_n - k_{n-2}). \tag{2.23}$$

Step 4. If $f(k)$ is satisfactorily small, the values k^2 can be regarded as a good approximation to λ_l, and so can $\overline{u}_{m,n}$ to its corresponding eigenfunction ϕ_l. Otherwise return back to Step 2. If $f(k)$ cannot diminish enough even through Steps 2–3 iteratively, suitably increase the term numbers, m and n, and go to Step 1 for a new trial.

3. Error bounds of eigenvalues

In the above algorithms, the magnitude as well as the error of $\lambda_{\min}(\mathbf{A})$ is an important criterion to measure the accuracy of numerical eigenvalues and eigenfunctions. This fact will be justified by a posteriori error analysis below. The eigenvalue problem (2.1) can be presented in a weak form: Seek $\lambda \in R$, $0 \neq u \in H_0^1(\Omega)$ such that

$$(\nabla u, \nabla v) = \lambda(u, v), \quad \forall v \in H_0^1(\Omega), \tag{3.1}$$

where $\nabla = (\partial/\partial x, \partial/\partial y)^{\mathrm{T}}$, and the Sobolev space $H_0^1(\Omega) = \{v | v \in H^1(\Omega), v|_\Gamma = 0\}$. Define a space H_0^* such that

$$H_0^* = \{v | v \in H^1(\Omega^+), v \in H^1(\Omega^-), v^+ = v^- \text{ in } \Gamma_0, v_v^+ = v_v^- \text{ in } \Gamma_0, v|_\Gamma = 0\}. \tag{3.2}$$

Problem (2.4) can also be written in a weak form: Seek $\lambda \in R$, $0 \neq u \in H_0^*$ such that

$$\langle \nabla u, \nabla v \rangle = \lambda(u, v), \quad \forall v \in H_0^1(\Omega), \tag{3.3}$$

where

$$\langle u, v \rangle = \int\int_{\Omega^+} uv \, \mathrm{d}\Omega + \int\int_{\Omega^-} uv \, \mathrm{d}\Omega. \tag{3.4}$$

From Hall and Porsching [10], we can prove the following lemma.

Lemma 3.1. *The weak forms* (3.1) *and* (3.3) *are equivalent to each other*, *and*

$$\langle \nabla\phi_i, \nabla\phi_j\rangle = (\nabla\phi_i, \nabla\phi_j) = \lambda\delta_{i,j}. \tag{3.5}$$

From Lemma 3.1, we conclude that any a function $v(\in H_0^*)$ can be expressed by the eigenfunctions $\{\phi_i\}$,[1] i.e.,

$$v = \sum_{i=1}^{\infty} \alpha_i \phi_i, \tag{3.6}$$

with the true expansion coefficients α_i. Suppose that there exist jumps ε_1 of v and ε_2 of v_ν, across the interface Γ_0, then the Helmholtz equation (2.5) is reduced to

$$\begin{cases} \Delta u + k^2 u = 0 & \text{in } \Omega^+ \quad \text{and} \quad \Omega^-, \\ [u]_{\Gamma_0} = \varepsilon_1, \qquad [u_\nu]_{\Gamma_0} = \varepsilon_2, \\ u|_\Gamma = g, \end{cases} \tag{3.7}$$

where the notation $[u]_{\Gamma_0} = (u^+ - u^-)|_{\Gamma_0}$. We use an auxiliary function w defined:

$$\begin{cases} \Delta w = 0, & \text{in } \Omega^+ \quad \text{and} \quad \Omega^-, \\ [w]_{\Gamma_0} = \varepsilon_1, \quad [w_\nu]_{\Gamma_0} = \varepsilon_2, \\ w|_\Gamma = g. \end{cases} \tag{3.8}$$

Note that function w is only for analysis but not for real computation. Now we have the following lemma.

Lemma 3.2. *Let* k^2 *be close to a target eigenvalue of* (2.1), *and let* u *and* w *be the solutions of* (3.7) *and* (3.8) *satisfying*[2]

$$|w|_{0,\Omega} \leqslant \tfrac{1}{2}\, |u|_{0,\Omega}. \tag{3.9}$$

Then there exists an eigenvalue λ_l such that

$$\frac{|k^2 - \lambda_l|}{k^2} \leqslant 2\frac{|w|_{0,\Omega}}{|u|_{0,\Omega}}. \tag{3.10}$$

Proof. Let $v = u - w$, then

$$\begin{cases} \Delta v + k^2 v = -k^2 w, & \text{in } \Omega^+ \quad \text{and} \quad \Omega^-, \\ [v]_{\Gamma_0} = 0, \qquad [v_\nu]_{\Gamma_0} = 0, \\ v|_\Gamma = 0. \end{cases} \tag{3.11}$$

So $v \in H_0^*$, and the function v can be expressed by (3.6). We obtain from (2.4), (3.11) and (3.6) that

$$|w|_{0,\Omega}^2 = \frac{1}{k^2}\, |\Delta v + k^2 v|_{0,\Omega}^2 = \sum_{i=1}^{\infty} \left(\frac{k^2 - \lambda_i}{k^2}\right)^2 \alpha_i^2. \tag{3.12}$$

Also from (2.3), (3.6) and assumption (3.9)

$$\sum_{i=1}^{\infty} \alpha_i^2 = |v|_{0,\Omega}^2 = |u - w|_{0,\Omega}^2 \geqslant (|u|_{0,\Omega} - |w|_{0,\Omega})^2 \geqslant \frac{1}{4}|u|_{0,\Omega}^2. \tag{3.13}$$

---

[1] In fact, when $v \in H_0^*$, we have $v^+ = v^-$ and $v^+ v_\nu^+ = v^- v_\nu^-$, to give $|v|_{1,\Omega^+}^2 + |v|_{1,\Omega^-}^2 = |v|_{1,\Omega}^2 + \int_{\Gamma_0} (v^+ v_\nu^+ - v^- v_\nu^-) = |v|_{1,\Omega}^2$. Hence $v \in H_0^*$ implies $v \in H_0^1(\Omega)$, and v can be expanded by the complete set of eigenfunctions $\phi_i (\in H_0^1(\Omega))$.

[2] When k^2 is close to a target eigenvalue, u is close to its corresponding eigenfunction. Hence $\varepsilon = \max\{g, \varepsilon_1, \varepsilon_2\}$ is small, and $|u|_{0,\Omega} = O(1)$ for some kinds of normalization. On the other hand, the maximal value of Laplace's solution w occurs only on the boundary, and then $|w|_{0,\Omega} \leqslant \varepsilon\, \text{Area}(\Omega)$. Hence assumption (3.9) can be provided.

Therefore, combining (3.12) and (3.13) yields

$$\min_i \left| \frac{k^2 - \lambda_i}{k^2} \right|^2 \leqslant \frac{\sum_{i=1}^{\infty} \left((k^2 - \lambda_i)/k^2\right)^2 \alpha_i^2}{\sum_{i=1}^{\infty} \alpha_i^2} \leqslant 4 \, \frac{|w|_{0,\Omega}^2}{|u|_{0,\Omega}^2}. \tag{3.14}$$

The desired bound (3.10) is obtained. This completes the Proof of Lemma 3.2. □

The bounds (3.10) can also be derived from Kuttler and Sigilloto [11] for the entire solution domain. We cite two lemmas from [17].

Lemma 3.3. *Suppose that the auxiliary function of* (3.8) *satisfies the following inverse properties*

$$|w_\nu|_{0,\Gamma} \leqslant K_w \|w\|_H, \quad |w_\nu^+|_{0,\Gamma_0} \leqslant K_w \|w\|_H, \quad \forall w \in H, \tag{3.15}$$

where the constant K_w may depend of w. Then for any $\sigma > 0$ there exists a constant C independent of w such that

$$\|w\|_H \leqslant C(K_w + \sigma^{-1})|w|_B. \tag{3.16}$$

Lemma 3.4. *Let u be the solution of* (2.5). *Then for $\sigma > 0$ there exists a unique function $u_{m,n} \in S_{m,n}$ by the TM such that*

$$|u_{m,n}|_B \leqslant |g|_{0,\Gamma}, \quad |u - u_{m,n}|_B \leqslant C \inf_{v \in S_{m,n}} |u - v|_B. \tag{3.17}$$

Now let us prove a new theorem.

Theorem 3.1. *Let u be the piecewise particular solution of the Helmholtz equation* (2.5). *Suppose that all conditions in Lemmas* 3.2 *and* 3.3 *hold. Then $\exists \lambda_l$ such that*

$$\frac{|k^2 - \lambda_l|}{k^2} \leqslant C(K_w + \sigma^{-1}) \, \frac{|u|_B}{|u|_{0,\Omega}}, \tag{3.18}$$

where C is a bounded constant independent of u. Moreover, let $u_{m,n} \in S_{m,n}$, then

$$\frac{|k^2 - \lambda_l|}{k^2} \leqslant C(K_w + \sigma^{-1}) \, \frac{|u_{m,n}|_B}{|u_{m,n}|_{0,\Omega}}. \tag{3.19}$$

Proof. From Lemmas 3.2 and 3.3 we obtain that

$$\frac{|k^2 - \lambda_l|}{k^2} \leqslant 2 \frac{|w|_{0,\Omega}}{|u|_{0,\Omega}} \leqslant 2 \, \frac{\|w\|_H}{|u|_{0,\Omega}} \leqslant C(K_w + \sigma^{-1}) \, \frac{|w|_B}{|u|_{0,\Omega}}. \tag{3.20}$$

Since the functions u and w have the same values on Γ and Γ_0 by comparing (3.7) with (3.8), the desired result (3.18) is obtained, and so is (3.19) by letting $u = u_{m,n}$. This completes the Proof of Theorem 3.1. □

It is worthy pointing out that the ratio in (3.19)

$$\rho = \frac{|u_{m,n}|_B}{|u_{m,n}|_{0,\Omega}} \tag{3.21}$$

plays an important role in error estimates for both eigenvalues and eigenfunctions. Note that $u_{m,n}$ solves the Helmholtz equation (2.5) under a given g on Γ. From Lemma 3.4 we directly have the following lemma.

Lemma 3.5. *Let $u_{m,n}(\in S_{m,n})$ be the solution to* (2.5) *from the TM. Suppose that there exists a constant $\rho_{10}(> 0)$ independent of m and n such that*

$$|u_{m,n}|_{0,\Omega} \geqslant \rho_{10}|c_1|, \tag{3.22}$$

where ρ_{10} *may depend of* k (*see Lemma* 5.1 *in Section* 5). *Then ratio* (3.21) *has the bounds*

$$\rho \leqslant \frac{1}{\rho_{10}} |\overline{u}_{m,n}|_B, \quad \rho \leqslant \frac{1}{\rho_{10}} \frac{1}{c_1} |g|_{0,\Gamma}, \tag{3.23}$$

where the scaled solution $\overline{u}_{m,n}$ *is given by* (2.17).

Let us consider the stiffness matrix $\mathbf{A}$ in (2.16). Denote the eigenvalues μ_i and eigenvectors $\bar{\mathbf{x}}_i$, then $\mathbf{A}\overline{\mathbf{x}}_\mathbf{i} = \mu_i \overline{\mathbf{x}}_\mathbf{i}$, where $0 < \mu_1 \leqslant \mu_2 \leqslant \cdots \leqslant \mu_N$, $N = m + n$, and $\overline{\mathbf{x}}_\mathbf{i}^T \overline{\mathbf{x}}_\mathbf{j} = \delta_{ij}$.

We can also prove the following lemma by following [2, p. 604].

Lemma 3.6. *Let* $\overline{\mathbf{x}}_{\mathbf{m},\mathbf{n}}$ *be the vector of the coefficients of the solution* $\overline{u}_{m,n}$ *in* (2.5) *by the TM using the least squares method. Suppose that* $\mu_1 = \lambda_{\min}(\mathbf{A}) \ll 1$, *the next minimal eigenvalue* $\mu_2 = \lambda_{\text{next}}(\mathbf{A}) = \mathrm{O}(1)$, *and* $\mathbf{x}_1$ *is the leading eigenvector of* $\mathbf{A}(k)$ *corresponding to* μ_1 *such that*

$$(\overline{\mathbf{x}}_{\mathbf{m},\mathbf{n}}, \mathbf{e}_1) = (\alpha \mathbf{x}_1, \mathbf{e}_1) = c_1 \neq 0, \tag{3.24}$$

where $\mathbf{e}_1$ *is the N-dimensional unit vector*, $\mathbf{e}_1 = (1, 0, \ldots, 0)^{\mathrm{T}}$. *Then there exist the bounds*

$$c_1 = \mathrm{O}\left(\frac{1}{\sqrt{\lambda_{\min}(\mathbf{A})}}\right), \tag{3.25}$$

and

$$\|\overline{\mathbf{x}}_{\mathbf{m},\mathbf{n}} - \alpha \mathbf{x}_1\| = \mathrm{O}\left(\sqrt{\frac{\lambda_{\min}(\mathbf{A})}{\lambda_{\text{next}}(\mathbf{A})}}\right), \tag{3.26}$$

with a suitable constant $\alpha \neq 0$.

Applying (3.19), (3.23) and (3.25) leads to the following corollary.

Corollary 3.1. *Let all conditions in Theorem* 3.1 *and Lemmas* 3.5 *and* 3.6 *hold. Then* $\exists \lambda_l$ *such that*

$$\left|\frac{k^2 - \lambda_l}{k^2}\right| \leqslant C \frac{(K_w + \sigma^{-1})}{\rho_{10}} |g|_{0,\Gamma} \sqrt{\lambda_{\min}(\mathbf{A})}. \tag{3.27}$$

Note that the function $g|_\Gamma$ in (2.5) may not be necessarily small. In fact, let $g = \mathrm{O}(1)$, we can still conclude that if $\lambda_{\min}(\mathbf{A}) \to 0$ then $k^2 \to \lambda_l$. Also the bounds of K_w can be derived by following [17,13] to give $K_w \leqslant C\sqrt{\max\{m, n\}}$ for a circular domain Ω^+.

4. Error bounds of eigenfunctions

In the algorithms in Section 2.2, the solution $\overline{u}_{m,n}$ in (2.17) by the TM can also be regarded as an approximation to the eigenfunctions ϕ_l. First, let us assume the distinct eigenvalues

$$0 < \lambda_1 < \lambda_2 < \cdots < \lambda_l < \cdots. \tag{4.1}$$

Also the values k^2 are chosen to be closer to a target eigenvalue λ_l. We provide the following lemma.

Lemma 4.1. *Let* u *and* w *be the solutions of* (3.7) *and* (3.8), *respectively, and suppose that*

$$|\lambda_i - \lambda_j| \geqslant \beta > 0, \quad i \neq j,$$

$$|w|_{0,\Omega} < \min\left\{\frac{1}{2}, \frac{\beta}{4k^2}\right\} |u|_{0,\Omega}. \tag{4.2}$$

Then there exists the bound,

$$|k^2 - \lambda_l| < \tfrac{1}{2}\beta. \tag{4.3}$$

Proof. From (4.2) and the first part of (3.20) we have

$$|k^2 - \lambda_l| = \min_i |k^2 - \lambda_i| = k^2 \min_i \frac{|k^2 - \lambda_i|}{k^2} \leqslant k^2 \frac{2|w|_{0,\Omega}}{|u|_{0,\Omega}} < \frac{\beta}{2}, \tag{4.4}$$

where we have used (3.10) under assumption (3.9). □

Theorem 4.1. *Let the conditions in Lemmas* 3.3 *and* 4.1 *hold. Then there exists a real constant* $a_l \neq 0$ *such that*

$$|u - a_l\phi_l|_{0,\Omega} \leqslant C\,\frac{\lambda_l}{\beta}(K_w + \sigma^{-1})|u|_B. \tag{4.5}$$

Proof. Let $v = u - w$, then v satisfies (3.11). The functions $v(\in H_0^*)$ can also be expressed by (3.6). Since the coefficients can be obtained explicitly from the orthogonality (3.5), we have

$$\alpha_i = -\frac{k^2}{k^2 - \lambda_i}(w, \phi_i). \tag{4.6}$$

Then the solution u of (3.7) is given by

$$\begin{aligned} u = w + v &= w - \sum_{i=1}^{\infty} \frac{k^2}{k^2 - \lambda_i}(w, \phi_i)\phi_i \\ &= w + a_l\phi_l - \sum_{i=1 \wedge i \neq l}^{\infty} \frac{k^2}{k^2 - \lambda_i}(w, \phi_i)\phi_i, \end{aligned} \tag{4.7}$$

where $a_l = \frac{-k^2}{k^2 - \lambda_l}(w, \phi_l)$. Since $\min_{i \neq l} |k^2 - \lambda_i| \geqslant \beta/2$, we obtain from (4.7) and the Parceval's inequality

$$\begin{aligned} |u - a_l\phi_l|_{0,\Omega} &\leqslant |w|_{0,\Omega} + \sqrt{\sum_{\substack{i=1 \\ i \neq l}}^{\infty} \left(\frac{k^2}{k^2 - \lambda_i}\right)^2 (w, \phi_i)^2} \\ &\leqslant |w|_{0,\Omega} + \frac{2k^2}{\beta}\sqrt{\sum_{i=1}^{\infty} (w, \phi_i)^2} \leqslant \left(1 + \frac{2k^2}{\beta}\right)|w|_{0,\Omega}. \end{aligned} \tag{4.8}$$

Also it follows from (4.3) that

$$k^2 \leqslant \lambda_l + |k^2 - \lambda_l| \leqslant \lambda_l + \frac{\beta}{2}. \tag{4.9}$$

Finally by applying (4.8), (4.9) and Lemma 3.3,

$$\begin{aligned} |u - a_l\phi_l|_{0,\Omega} &\leqslant C\,\frac{\lambda_l}{\beta}|w|_{0,\Omega} \leqslant C\frac{\lambda_l}{\beta}\,\|w\|_H \\ &\leqslant C\,\frac{\lambda_l}{\beta}(K_w + \sigma^{-1})|w|_B = C\,\frac{\lambda_l}{\beta}(K_w + \sigma^{-1})|u|_B. \end{aligned} \tag{4.10}$$

This completes the Proof of Theorem 4.1. □

Theorem 4.2. *Let all conditions in Theorem* 4.1 *hold. Then there exists a real constant* a_l *such that*

$$\|u - a_l\phi_l\|_H \leq C\,\frac{\lambda_l^{3/2}}{\beta}(K_w + \sigma^{-1})|u|_B. \tag{4.11}$$

Proof. Let $v = u - a_l\phi_l$, we have from (3.7), (2.4) and (2.5)

$$\begin{aligned}|v|_H^2 &\leqslant \langle -\Delta v, v\rangle + C(K_w + \sigma^{-1})^2|v|_B^2\\ &= (k^2u - \lambda_l a_l\phi_l, v) + C_1(K_w + \sigma^{-1})^2|v|_B^2\\ &= (\lambda_l v + (k^2 - \lambda_l)u, v) + C_1(K_w + \sigma^{-1})^2|v|_B^2,\end{aligned} \tag{4.12}$$

where we have used $a_l\phi_l = u - v$, and C_1 is a constant. Then we obtain

$$|v|_H^2 \le \lambda_l|v|_{0,\Omega}^2 + |k^2 - \lambda_l||u|_{0,\Omega}|v|_{0,\Omega} + C(K_w + \sigma^{-1})^2|v|_B^2. \tag{4.13}$$

Moreover from Theorem 3.1,

$$|k^2 - \lambda_l||u|_{0,\Omega} \le k^2(K_w + \sigma^{-1})|u|_B. \tag{4.14}$$

Consequently, we can conclude from (4.13) and (4.14) and $|u|_B = |v|_B$ that

$$\begin{aligned}\|v\|_H^2 &= |v|_{0,\Omega}^2 + |v|_H^2\\ &\le (1+\lambda_l)|v|_{0,\Omega}^2 + k^2(K_w + \sigma^{-1})|u|_B|v|_{0,\Omega} + C(K_w + \sigma^{-1})^2|v|_B^2.\end{aligned} \tag{4.15}$$

From Theorem 4.1

$$|v|_{0,\Omega} = |u - a_l\phi_l|_{0,\Omega} \leqslant C\frac{\lambda_l}{\beta}(K_w + \sigma^{-1})|u|_B. \tag{4.16}$$

Eq. (4.15) is reduced to

$$\|v\|_H^2 \le C\left\{(1+\lambda_l)\left(\frac{\lambda_l}{\beta}\right)^2(K_w + \sigma^{-1})^2 + k^2(K_w + \sigma^{-1})^2\frac{\lambda_l}{\beta}\right\}\quad |u|_B^2. \tag{4.17}$$

The desired results (4.11) are obtained immediately by noting $v = u - a_l\phi_l$. This completes the Proof of Theorem 4.1. □

Corollary 4.1. *Suppose that all the conditions in Theorem* 4.1 *hold*, *and let* $u(=u_{m,n} \in S_{m,n})$ *be the solution of* (2.5) *by the TM*. *Then there exists the true* $a_l \ne 0$ *such that*

$$\frac{|u_{m,n} - a_l\phi_l|_{0,\Omega}}{|u_{m,n}|_{0,\Omega}} \le C\frac{\lambda_l}{\beta}(K_w + \sigma^{-1})\frac{|u_{m,n}|_B}{|u_{m,n}|_{0,\Omega}}, \tag{4.18}$$

and

$$\frac{\|u_{m,n} - a_l\phi_l\|_H}{|u_{m,n}|_{0,\Omega}} \le C\frac{\lambda_l^{3/2}}{\beta}(K_w + \sigma^{-1})\frac{|u_{m,n}|_B}{|u_{m,n}|_{0,\Omega}}. \tag{4.19}$$

Compared with (3.19), the error bounds (4.18) and (4.19) for eigenfunctions contain the same ratios ρ of (3.21). Therefore, other results as to (3.27) can be similarly provided from Corollary 4.1, Lemmas 3.5 and 3.6.

To close this section, we consider the eigenvalues with multiplicity $r \geqslant 1$:

$$\cdots < \lambda_{l-1} < \lambda_l = \lambda_{l+1} = \cdots = \lambda_{l+r-1} < \lambda_{l+r} < \cdots. \tag{4.20}$$

Moreover, we assume that all eigenfunctions are distinct. By similar arguments as above, we can conclude that there exists a linear combination of the eigenfunctions, $\phi_l, \phi_{l+1}, \ldots, \phi_{l+r-1}$, such that $\phi_l^* = \sum_{j=0}^{r-1} a_{l+j}\phi_{l+j}$, with coefficients a_{l+j}. There also exist the error bounds,

$$\frac{|u_{m,n} - \phi_l^*|_{0,\Omega}}{|u_{m,n}|_{0,\Omega}} \le C\frac{\lambda_l}{\beta}(K_w + \sigma^{-1})\frac{|u_{m,n}|_B}{|u_{m,n}|_{0,\Omega}}, \tag{4.21}$$

and

$$\frac{\|u_{m,n}-\phi_l^*\|_H}{|u_{m,n}|_{0,\Omega}} \le C\,\frac{\lambda_l^{3/2}}{\beta}(K_w+\sigma^{-1})\,\frac{|u_{m,n}|_B}{|u_{m,n}|_{0,\Omega}}. \tag{4.22}$$

5. Numerical experiments

5.1. A basic model

Let us consider a simple eigenvalue problem (see Fig. 1)

$$\begin{cases}\Delta u+\lambda u=0 & \text{in } \Omega^*,\\ u|_\Gamma=0,\end{cases} \tag{5.1}$$

where Ω^* is the square solution domain $\{(x, y)| -1 < x < 1, -1 < y < 1\}$. The corresponding Helmholtz equation is

$$\begin{cases}\Delta u+k^2 u=0 & \text{in } \Omega^*,\\ u|_\Gamma=1.\end{cases} \tag{5.2}$$

For simplicity, based on symmetry we may seek the solution only in Ω, one eighth of Ω^* (see Fig. 2)

$$\begin{cases}\Delta u+k^2 u=0 & \text{in } \Omega,\\ u_\nu|_{\overline{AC}}=0, u_\nu|_{\overline{AB}}=0,\\ u|_{\overline{BC}}=1.\end{cases} \tag{5.3}$$

Choose the admissible functions

$$v_m=\sum_{i=0}^{m}\hat{c}_i J_i(kr)\cos i\theta, \quad m=4M-1, \tag{5.4}$$

where $\hat{c}_i$ are the coefficients to be sought, (r, θ) are the polar coordinates with the origin O, and $J_i(z)$ is the Bessel functions defined by [1]

$$J_\mu(r)=\sum_{i=1}^{\infty}\frac{(-1)^i}{\Gamma(i+1)\Gamma(i+\mu+1)}\left(\frac{r}{2}\right)^{2i+\mu}. \tag{5.5}$$

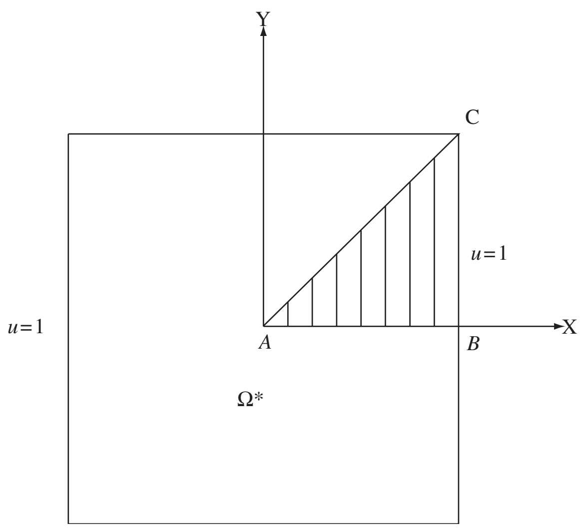

Fig. 1. The entire solution domain.

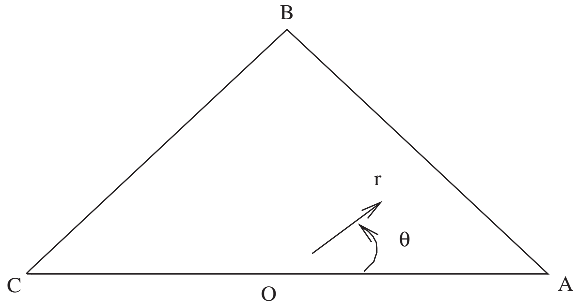

Fig. 2. One-eighth of Fig. 1 in Partition I.

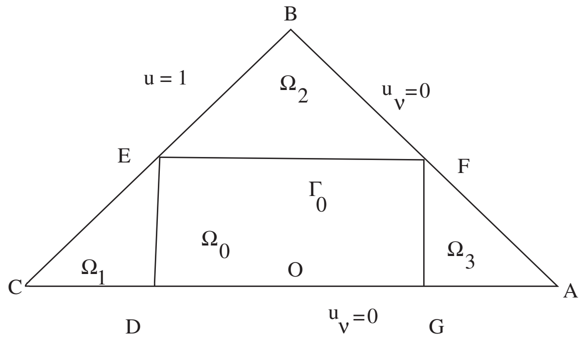

Fig. 3. One-eighth of Fig. 1 in Partition II.

Based on the study in [15], the partition, $\Omega = \Omega_0 \cup \Omega_1 \cup \Omega_2 \cup \Omega_3$, of Ω is beneficial to numerical stability, where the interface Γ_0 is composed of the piecewise straight lines shown in Figs. 3 and 4. The piecewise particular solutions can be found as follows:

$$\begin{cases} v_m^{(0)} = \sum_{i=0}^{m} \hat{c}_i J_i(kr) \cos i\theta & \text{in} \quad \Omega_0, \quad m = 4M - 1, \\ v_k^{(1)} = 1 + \sum_{i=0}^{K} \hat{d}_i J_{2(2i+1)}(k\rho) \sin 2(2i+1)\phi & \text{in} \quad \Omega_1, \\ v_n^{(2)} = 1 + \sum_{i=0}^{N} \hat{b}_i J_{2i+1}(k\xi) \sin(2i+1)w & \text{in} \quad \Omega_2, \\ v_l^{(3)} = \sum_{i=0}^{L} \hat{a}_i J_{4i}(k\eta) \cos 4i\psi & \text{in} \quad \Omega_3. \end{cases} \tag{5.6}$$

In (5.6) $\hat{a}_i, \hat{b}_i, \hat{c}_i, \hat{d}_i$ are the unknown coefficients, and (r, θ), (ρ, ϕ), (ξ, w) and (η, ψ) are the polar coordinates at the origins O, C, B, A, respectively. Note that for the non-homogeneous boundary condition $u|_\Gamma = 1$, there exists a mild singularity $O(\rho^2 \ln \rho)$ at the corner C (i.e., the corners in Fig. 4), and some singular solutions should be added for solving the Helmholtz equation exactly (see [15]). However for the homogeneous boundary condition $u|_\Gamma = 0$, such a mild singularity does not exist. Since for the eigenvalue problem, only the homogeneous Dirichlet conditions are involved, we ignore the singular functions given in [15], which have no effects on the stiffness matrix **A**.

The division in Fig. 3 (also see Fig. 4) using the piecewise particular solutions in (5.6) is called Partition II of the TM; and the division in Fig. 1 using (5.4) for the entire solution domain is called Partition I of the TM.

Let us give a lemma for supporting assumption (3.22), whose proof is omitted.

Lemma 5.1. *Let a semi-circus $S_{r_0}(0 \le r \le r_0, 0 \le \theta \le \pi)$ be included in Ω_0, and choose* (5.6) *as the admissible functions*, $u_{m,n} \in S_{m,n}$. *Then there exist the bounds*

$$|u_{m,n}|_{0,\Omega} \geqslant \min\left\{\frac{1}{2}r_0, \frac{1}{3}\frac{1}{k}\right\} |\hat{c}_0|. \tag{5.7}$$

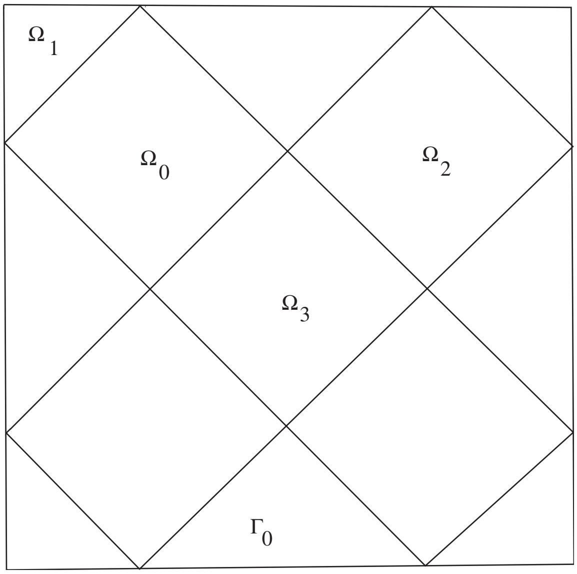

Fig. 4. Partition II to the entire solution domain.

5.2. Expansions of eigenfunctions

Take model (5.1) as an example in computation. The eigenvalues and eigenfunctions are known as

$$\lambda_{i,j} = \frac{\pi^2}{4}[(2i-1)^2 + (2j-1)^2], \quad u_{i,j} = \cos\frac{(2i-1)\pi}{2}x\cos\frac{(2j-1)\pi}{2}y. \tag{5.8}$$

Below, let us provide the expansions of $\hat{u}_{l,l}$ by means of the Bessel functions (5.5). Denote

$$\hat{k} = \sqrt{\lambda_{l,l}} = \frac{\pi}{\sqrt{2}}(2l-1), \ \ l = 1, 2, \ldots, \quad \hat{u}_{l,l} = \cos\frac{\hat{k}}{\sqrt{2}}x\cos\frac{\hat{k}}{\sqrt{2}}y. \tag{5.9}$$

We can prove the following lemma (see [14]).

Lemma 5.2. *The eigenfunctions in* (5.9) *can be expressed as the following expansions*:

$$\begin{cases} \hat{u}_{l,l} = J_0(kr) + 2\sum_{i=1}^{\infty} J_{2i}(\hat{k}r)\cos(2i+1)\theta \\ \qquad +2(-1)^{l+1}\sum_{i=0}^{\infty}(-1)^i J_{2i+1}(\hat{k}r)\cos(2i+1)\theta \quad \text{in } \Omega_0, \\ \hat{u}_{l,l} = 4\sum_{i=0}^{\infty}(-1)^i J_{4i+2}(\hat{k}\rho)\sin(4i+2)\psi \quad \text{in } \Omega_1, \\ \hat{u}_{l,l} = 2\sqrt{2}(-1)^{l+1}\sum_{i=0}^{\infty}(-1)^{\lfloor (i+1)/2\rfloor} J_{2i+1}(\hat{k}\xi)\sin(2i+1)w \quad \text{in } \Omega_2, \\ \hat{u}_{l,l} = 2J_0(\hat{k}\eta) + 4\sum_{i=1}^{\infty}(-1)^i J_{4i}(\hat{k}\eta)\cos 4i\psi \quad \text{in } \Omega_3, \end{cases} \tag{5.10}$$

where $\lfloor i/2 \rfloor$ *is the floor function of* $i/2$.

Comparing Lemma 5.2 with (5.6), the solutions $\hat{u}_{l,l}$ with even l have the following, simple true coefficients

$$\begin{cases} \{\hat{c}_i\} : 1, 2, 2, -2, 2, 2, 2, -2, \ldots \\ \{\hat{a}_i\} : 2, -4, 4, -4, 4, 4, -4, 4, -4, \ldots \\ \{\hat{b}_i\} : 2\sqrt{2}, -2\sqrt{2}, -2\sqrt{2}, 2\sqrt{2}, 2\sqrt{2}, -2\sqrt{2}, -2\sqrt{2}, 2\sqrt{2}, \ldots \\ \{\hat{d}_i\} : 4, -4, 4, -4, 4, -4, 4, -4, \ldots. \end{cases} \tag{5.11}$$

Since the leading coefficient $c_0 = 1$, the errors of computed eigenfunctions can be easily discovered from (5.11).

5.3. Numerical results

In computation, it is better to choose the scaled forms of (5.4)

$$v_m = \sum_{i=0}^{4M-1} c_i \frac{J_i(kr)}{J_i(kr_0)} \cos i\theta, \tag{5.12}$$

where $r_0 = \frac{1}{2}$ and $J_i(kr_0) \neq 0$ in computation. Hence $\hat{c}_i = c_i / J_i(kr_0)$. The admissible functions (5.12) already satisfy the Helmholtz equation in Ω and the boundary condition $u_v|_{\overline{AC}} = 0$. Hence the coefficients c_i should be chosen to satisfy the remaining boundary conditions in (5.3) only. Define a quadratic functional

$$I(c_i) = \int_{\overline{BC}} (v-1)^2 \, \mathrm{d}l + \sigma^2 \int_{\overline{AB}} v_v^2 \, \mathrm{d}l, \tag{5.13}$$

where $\sigma = 1/4M$. The TM in Partition I is designed by seeking the coefficients c_i such that

$$I(\tilde{c}_i) = \min_{c_i} I(c_i). \tag{5.14}$$

The boundary errors are defined by

$$|\varepsilon|_B = |\varepsilon|_I = (|\varepsilon|^2_{0,\overline{BC}} + \sigma^2 |\varepsilon_v|^2_{0,\overline{AB}})^{1/2}, \tag{5.15}$$

where $\varepsilon = u - u_m$.

For Partition II, the continuity conditions across Γ_0 should be added to (5.3), thus to give

$$\begin{cases} \Delta u + k^2 u = 0 & \text{in } \Omega_0, \Omega_1, \Omega_2, \Omega_3, \\ u^+ = u^-, \ \dfrac{\partial u^+}{\partial v} = \dfrac{\partial u^-}{\partial v} & \text{on } \Gamma_0, \\ \dfrac{\partial u}{\partial v}|_{\overline{AC}} = \dfrac{\partial u}{\partial v}|_{\overline{AB}} = 0, & \\ u|_{\overline{BC}} = 1. & \end{cases} \tag{5.16}$$

Similarly, the admissible functions (5.6) should be scaled by

$$\begin{cases} v_m^{(0)} = \sum_{i=0}^{4M-1} c_i \dfrac{J_i(kr)}{J_i(kr_0)} \cos i\theta & \text{in } \Omega, \\ v_k^{(1)} = 1 + \sum_{i=0}^{K} d_i \dfrac{J_{2(2i+1)}(k\rho)}{J_{2(2i+1)}(k\rho_0)} \sin 2(2i+1)\phi & \text{in } \Omega_1, \\ v_m^{(2)} = 1 + \sum_{i=0}^{N} b_i \dfrac{J_{2i+1}(k\xi)}{J_{2i+1}(k\xi_0)} \sin(2i+1)w & \text{in } \Omega_2, \\ v_m^{(3)} = \sum_{i=0}^{L} a_i \dfrac{J_{4i}(k\eta)}{J_{4i}(k\eta_0)} \cos 4i\psi & \text{in } \Omega_3, \end{cases} \tag{5.17}$$

where $r_0 = \rho_0 = \psi_0 = \eta_0 = \frac{1}{2}$ in computation, and all the denominators in (5.17) are assumed to be nonzero. There exist the following relations between the coefficients,

$$\hat{c}_i = \frac{c_i}{J_i(kr_0)}, \quad \hat{d}_i = \frac{d_i}{J_{2(2i+1)}(k\rho_0)}, \quad \hat{b}_i = \frac{b_i}{J_{2i+2}(k\xi_0)}, \quad \hat{a}_i = \frac{a_i}{J_{4i}(k\eta_0)}. \tag{5.18}$$

The admissible functions (5.17) satisfy the Helmholtz equations in Ω_i and the exterior boundary in $\partial\Omega$ already. Hence, the TM in Partition II is designed for seeking the coefficients a_i, b_i, c_i, d_i to minimize the functional

$$I_2(\tilde{a}_i, \tilde{b}_i, \tilde{c}_i, \tilde{d}_i) = \min_{a_i, b_i, c_i, d_i} I_2(a_i, b_i, c_i, d_i), \tag{5.19}$$

Table 1
The iteration solutions of $\lambda_{2,2}$ for (a) Partition I ($M=3$) and (b) Partition II ($L=M=K=3$, $N=5$)

n	$\sqrt{\tilde{\lambda}_{2,2}^{(n)}}$	$\Delta\sqrt{\tilde{\lambda}_{2,2}^{(n)}}$	$\lambda_{\min}(\mathbf{A})$	$\|\varepsilon\|_{\mathrm{I}}$	Cond.	$\sqrt{\dfrac{\lambda_{\min}(\mathbf{A})}{\lambda_{\mathrm{next}}(\mathbf{A})}}$
(a)						
1	6.5		0.190 (−2)			
2	6.51		0.168 (−2)			
3	6.52		0.147 (−2)			
4	6.6667792506	0.246 (−2)	0.429 (−6)	0.283 (−2)	2.06 (4)	0.174 (−2)
5	6.6650330025	0.709 (−3)	0.358 (−7)	0.805 (−3)	7.11 (4)	0.503 (−3)
6	6.6643113338	0.131 (−4)	0.947 (−10)	0.381 (−3)	1.38 (6)	0.259 (−4)
7	6.6643245328	0.126 (−6)	0.824 (−10)	0.375 (−3)	1.48 (6)	0.241 (−4)
8	6.6643244951	0.879 (−7)	0.824 (−10)	0.388 (−3)	1.48 (6)	0.241 (−4)
9	6.6643238340	0.573 (−6)	0.824 (−10)	0.987 (−3)	1.48 (6)	0.241 (−4)
10	6.6643242774	0.130 (−6)	0.824 (−10)	0.988 (−3)	1.48 (6)	0.241 (−4)
(b)						
1	6.5		0.426 (−3)			
2	6.51		0.379 (−3)			
3	6.52		0.334 (−3)			
4	6.7032345641	0.389 (−1)	0.283 (−4)	0.323 (−2)	369.	0.0995
5	6.6692226997	0.490 (−2)	0.436 (−6)	0.450 (−3)	2.89 (3)	0.0124
6	6.6616269133	0.270 (−3)	0.132 (−6)	0.254 (−3)	5.24 (3)	0.678 (−2)
7	6.6643544781	0.301 (−4)	0.164 (−10)	0.291 (−5)	4.71 (5)	0.757 (−4)
8	6.6643188680	0.554 (−5)	0.566 (−12)	0.521 (−6)	2.53 (6)	0.141 (−4)
9	6.6643243807	0.265 (−7)	0.107 (−13)	0.279 (−5)	1.84 (7)	0.193 (−5)
10	6.6643244076	0.357 (−9)	0.107 (−13)	0.417 (−5)	1.84 (7)	0.194 (−5)

where $I_2(\tilde{a}_i, \tilde{b}_i, \tilde{c}_i, \tilde{d}_i)$ involves only the interior boundary conditions, given by

$$I_2(\tilde{a}_i, \tilde{b}_i, \tilde{c}_i, \tilde{d}_i) = \int_{\Gamma_0} (v^+ - v^-)^2 \, \mathrm{d}l + \sigma^2 \int_{\Gamma_0} (v_\nu^+ - v_\nu^-)^2 \, \mathrm{d}l, \tag{5.20}$$

and $\sigma = 1/\max(4M, 4K+2, 2N+1, 4L)$. Also the boundary errors are

$$|\varepsilon|_{\mathrm{II}} = (|v^+ - v^-|^2_{0,\Gamma_0} + \sigma^2 |u_\nu^+ - u_\nu^-|^2_{0,\Gamma_0})^{1/2}. \tag{5.21}$$

Since the minimal eigenvalue and its corresponding eigenfunction have been investigated in [14] of this model already, in this paper, we will apply the algorithms in Section 2 to seek $\lambda_{2k,2k}$ and $\tilde{u}_{2k,2k}$, $k = 1, 2, \ldots$. For $\lambda_{2,2}$, the initial values of k are chosen as $k_0 = 6.5$, $k_1 = 6.51$, $k_2 = 6.52$. Numerical solutions have been obtained with about 10 iterations, and listed in Tables 1 and 2. Since the relative errors

$$\delta = \left| \frac{k^2 - \lambda_l}{k^2} \right| \approx \frac{2}{k} \Delta\tilde{\lambda}_l \quad \text{as} \quad k \to \lambda_l, \tag{5.22}$$

we can evaluate from Table 1 that $\delta \approx 4 \times 10^{-8}$ and $\delta \approx 5 \times 10^{-11}$ at the tenth iteration for Partition I and II, respectively.

Comparing the coefficients $\hat{c}_i$ etc. in Table 2 with the true values in (5.11), the following coefficient errors $\Delta\hat{c}_i$ etc. can be observed

$$\Delta\hat{c}_0 = 0, \quad \Delta\hat{c}_i = \mathrm{O}(10^{-3}), \quad i = 1, 2, 3, 4$$

Table 2
The calculated coefficients at the 10th iteration of $\lambda_{2,2}$ for (a) Partition I ($M=3$) and (b) Partition II ($L=M=K=3$, $N=5$), where $c_i=\hat{c}_i/J_i(k/2)/\hat{c}_0/J_0(k/2)$, $a_i=\hat{a}_i/J_{4i}(k/2)/\hat{c}_0/J_0(k/2)$, $b_i=\hat{b}_i/J_{2i+1}(k/2)/\hat{c}_0/J_0(k/2)$, $d_i=\hat{d}_i/J_{4i+2}(k/2)/\hat{c}_0/J_0(k/2)$

i	$\hat{c}_i$	c_i
(a)		
0	−0.95619748 (3)	1.00000000
1	−0.11305572 (4)	−2.00195468
2	0.25927238 (4)	2.00186645
3	0.19820519 (4)	2.00205952
4	0.97612797 (3)	2.00236195
5	−0.36094094 (3)	−2.00101585
6	0.10781086 (3)	2.00244818
7	0.27021200 (2)	1.99980194
8	0.58890895 (1)	2.00946683
9	−0.11268614 (1)	−2.01130915
10	0.19365346	2.02112074
11	0.29412495 (−1)	1.98332728
(b)		
0	−0.52528202 (5)	1.00000000
1	−0.62046747 (5)	−2.00006037
2	0.14230026 (6)	2.00005406
3	0.10877407 (5)	2.00005951
4	0.53560610 (5)	2.00002638
5	−0.19817038 (5)	−1.99989163
6	0.59139322 (4)	1.99952794
7	0.14860825 (4)	2.00205815
8	0.32059004 (3)	1.99128394
9	−0.60473551 (2)	−1.96482272
10	0.97431101 (1)	1.85102922
11	0.20891285 (1)	2.56433910
i	$\hat{a}_i$	$.a_i$
0	−0.10506037 (6)	2.00007559
1	−0.10712071 (6)	−4.00003377
2	0.64399398 (3)	4.00004584
3	−0.47412716	−4.11594336
i	$\hat{b}_i$	$.b_i$
0	−0.87746737 (5)	−2.82824927
1	0.15382803 (6)	2.82847929
2	0.28028332 (5)	2.82855724
3	−0.20993087 (4)	−2.82819972
4	−0.86653283 (2)	−2.81541823
5	0.26238770 (1)	3.22072597
i	$\hat{d}_i$	$.d_i$
0	0.28459973 (6)	4.00009709
1	−0.11844975 (5)	−4.00484102
2	0.21303647 (2)	4.04733943
3	−0.10016769 (1)	−5.53818749 (2)

for Partition I, and

$$\Delta\hat{c}_0=0,\quad \Delta\hat{c}_i=\mathrm{O}(10^{-4}),\quad i=1,2,3,4,$$

$$\Delta\hat{a}_0=\mathrm{O}(10^{-4}),\quad \Delta\hat{b}_0=\mathrm{O}(10^{-4}),\quad \Delta\hat{d}_0=\mathrm{O}(10^{-4}),$$

for Partition II. Evidently, Partition II has a better performance. For $\tilde{\lambda}_{6,6}$ and $\tilde{u}_{6,6}$, the results are provided in Table 3.

Table 3
The approximate eigenvalues $\tilde{\lambda}_{6,6}$ and other results for Partitions I and II

M	$\sqrt{\tilde{\lambda}_{6,6}}$	$\Delta\sqrt{\tilde{\lambda}_{6,6}}$	$\lambda_{\min}(\mathbf{A})$	$\|\varepsilon\|_{\mathrm{I}}$	Cond.	Δc_2^*
4	24.22245279	0.213	0.753 (−2)	0.0297	96.4	0.714
5	24.43569090	0.165 (−3)	0.811 (−4)	0.0492	1.22 (4)	0.138
6	24.43585345	0.271 (−5)	0.206 (−7)	0.192 (−2)	1.02 (6)	0.0932
7	24.43584108	0.151 (−5)	0.752 (−11)	0.176 (−5)	4.89 (7)	0.255 (−3)

L	M	N	K	$\sqrt{\tilde{\lambda}_{6,6}}$	$\Delta\sqrt{\tilde{\lambda}_{6,6}}$	$\lambda_{\min}(\mathbf{A})$	$\|\varepsilon\|_{\mathrm{I}}$	Cond.	Δc_2^*	Δa_0^*
3	3	5	3	24.48826656	0.524 (−1)	0.548 (−2)	5.31	1.08 (3)	6.20	21.7
4	4	7	4	24.43595816	0.102 (−4)	0.613 (−5)	0.299 (−1)	7.83 (4)	0.114	0.311
5	5	9	5	24.43585339	0.223 (−6)	0.370 (−9)	0.117 (−2)	9.46 (6)	0.543 (−2)	0.157 (−1)
6	6	11	6	24.43585558	0.584 (−6)	0.947 (−12)	0.225 (−6)	1.81 (8)	0.245 (−5)	0.703 (−5)

Table 4
The calculated results for $\tilde{\lambda}_{l,l}$ for Partitions I and II

l	M	$\sqrt{\tilde{\lambda}_{l,l}}$	$\Delta\sqrt{\tilde{\lambda}_{l,l}}$	$\lambda_{\min}(\mathbf{A})$	$\|\varepsilon\|_{\mathrm{I}}$	Cond.
1	2	2.2214414879	0.191 (−7)	0.298 (−11)	0.242 (−4)	2.99 (6)
2	3	6.6643242774	0.129 (−6)	0.824 (−10)	0.988 (−3)	1.48 (6)
3	4	11.10720797	0.628 (−6)	0.135 (−10)	0.546 (−4)	9.77 (6)
6	7	24.43584108	0.151 (−5)	0.752 (−11)	0.176 (−5)	1.02 (9)
10	10	42.20738481	0.310 (−5)	0.562 (−10)	0.194 (−4)	4.89 (7)

l	L	M	N	K	$\sqrt{\tilde{\lambda}_{l,l}}$	$\Delta\sqrt{\tilde{\lambda}_{l,l}}$	$\lambda_{\min}(\mathbf{A})$	$\|\varepsilon\|_{\mathrm{II}}$	Cond.
1	2	2	3	2	2.2214414716	0.251 (−8)	0.471 (−14)	0.970 (−6)	3.13 (7)
2	3	3	5	3	6.6643224076	0.357 (−9)	0.107 (−13)	0.417 (−5)	1.84 (7)
3	4	4	7	4	11.10722750	0.158 (−6)	−0.273 (−13)	0.419 (−7)	8.10 (8)
6	7	7	13	7	24.43585593	0.226 (−6)	0.199 (−14)	0.752 (−8)	3.85 (8)
10	10	10	19	10	42.20738867	0.754 (−6)	0.218 (−14)	0.361 (−7)	1.47 (9)

Finally we have obtained the solutions for $\lambda_{l,l}$ and $u_{l,l}$ with $l = 1, 2, 3, 6, 10$, and listed in Table 4. When $l = 10$, $k \approx \sqrt{\tilde{\lambda}_{10,10}} \approx 42.2 \approx 7(2\pi)$, the relative errors in the approximate eigenvalue $\tilde{\lambda}_{10,10}$ with $\delta \approx 1.5 \times 10^{-7}$ and $\delta \approx 3.5 \times 10^{-8}$ have been obtained by using 39 particular solutions in Partition I and 83 piecewise particular solutions in Partitions II, respectively. Note that the algorithms in this paper work well for the repeated eigenvalue $\lambda_{3,3}$, where $\lambda_{3,3} = \lambda_{1,4} = 25.5\pi^2$, with the relative errors $\delta \approx 1.1 \times 10^{-7}$ and $\delta \approx 2.8 \times 10^{-8}$ for Partitions I and II, respectively. Evidently, Partition II using piecewise particular solutions may yield a higher accuracy than that by Partition I.

5.4. The crack eigenvalue problem

Finally, let us consider a new eigenvalue problem for the crack problem with singularity (see Fig. 5)

$$\begin{cases} -\Delta u = \lambda u & \text{in } \Omega, \\ u = 0 & \text{on } \overline{AB} \cup \overline{BC} \cup \overline{CD} \cup \overline{DO}, \\ u_\nu = 0 & \text{on } \overline{OA}, \end{cases} \tag{5.23}$$

where $\Omega = (-1, 1) \times (0, 1)$. We may seek the Helmholtz problem

$$\begin{cases} -\Delta u = k^2 u & \text{in } \Omega, \\ u = 1 & \text{on } \overline{AB} \cup \overline{BC} \cup \overline{CD}, \quad u = 0 \quad \text{on } \overline{DO}, \\ u_\nu = 0 & \text{on } \overline{OA}. \end{cases} \tag{5.24}$$

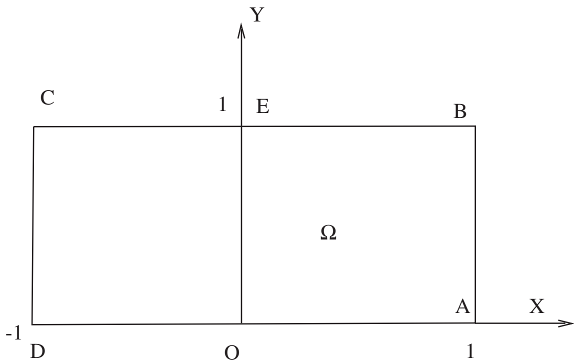

Fig. 5. The crack problem.

The particular solutions are given by

$$v^+ = \sum_{i=1}^{\infty} \hat{c}_i J_{i-\frac{1}{2}}(kr) \cos\left(i - \frac{1}{2}\right)\theta, \tag{5.25}$$

where $\hat{c}_i$ are expansion coefficients. In computation, we choose

$$v^+ = \sum_{i=1}^{L} c_i \frac{J_{i-1/2}(kr)}{J_{i-1/2}(kr_0)} \cos\left(i - \frac{1}{2}\right)\theta, \tag{5.26}$$

where the parameter r_0 is chosen to be $r_0 = 1$. There exist the following relations between $\hat{c}_i$ and c_i

$$\hat{c}_i = \frac{c_i}{J_{i-\frac{1}{2}}(kr_0)}. \tag{5.27}$$

For Step 1 of the iterative algorithms in Section 2.2, a good initial guess of $\sqrt{\lambda_{\min}}$ (or $\sqrt{\lambda_{\text{next}}}$) is important to the convergence of the iteration algorithm. Let us derive a lower bound of $\lambda_{\min}$. First consider an auxiliary eigenvalue problem,

$$\begin{cases} -\Delta u = \lambda u, & \text{in } \hat{S}, \\ u = 0, & \text{on } \partial\hat{S}, \end{cases} \tag{5.28}$$

where $\hat{S} = \{(x, y) | -1 < x < 1, -1 < y < 1\}$. The eigenfunctions of (5.28) are

$$u = \cos\left\{\frac{(2i-1)\pi}{2} x\right\} \cos\left\{\frac{(2j-1)\pi}{2} y\right\}. \tag{5.29}$$

Hence the minimal eigenvalue is found as

$$\hat{\lambda}_{\min} = \frac{\pi^2}{2}. \tag{5.30}$$

In fact, the crack problem in (5.23) has more the Dirichlet condition on a section $\overline{OD}$ in Fig. 5. Hence based on the variational description of the eigenvalue problems in [6], the minimal eigenvalue of problem (5.23) will not decline when the admissible functions are constrained under this Dirichlet condition:

$$\frac{\pi^2}{2} = \hat{\lambda}_{\min} \leqslant \lambda_{\min}. \tag{5.31}$$

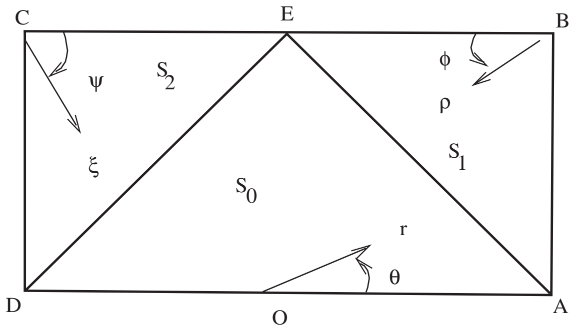

Fig. 6. A partition for the crack eigenvalue problem.

Next, consider the other auxiliary eigenvalue problem on $S^+ = (-1,1) \times (-\frac{1}{2}, \frac{1}{2})$ with the Dirichlet condition on the entire boundary ∂S^+. Since the eigenfunctions are

$$u = \cos\left\{\frac{(2i-1)\pi}{2} x\right\} \cos(2j-1)\pi y, \tag{5.32}$$

the minimal eigenvalue is given by

$$\lambda^+_{\min} = \frac{\pi^2}{4} + \pi^2 = \frac{5}{4}\pi^2. \tag{5.33}$$

For the crack eigenvalue problem (5.23),[3] there also exists the Neumann condition on $\overline{OA}$, a part of ∂S^+ (see Fig. 5). Hence from [6] again, when this Neumann condition is changed to the Dirichlet condition of the other auxiliary problem, the minimal eigenvalue of this problem will not decline, either. Then, we have the upper bound

$$\lambda_{\min} \leqslant \lambda^+_{\min} = \frac{5}{4}\pi^2. \tag{5.34}$$

Combining (5.30) and (5.34) gives

$$\frac{\pi^2}{2} \leqslant \lambda_{\min} \leqslant \frac{5}{4}\pi^2, \quad \frac{\pi}{\sqrt{2}} \leqslant \sqrt{\lambda_{\min}} \leqslant \frac{\sqrt{5}}{2}\pi. \tag{5.35}$$

Based on the bound of (5.35), we may easily find a good initial value (as well as three good initial values) of k for $\sqrt{\lambda_{\min}}$. By increasing k, we can find a good initial value of k for $\sqrt{\lambda_{\text{next}}}$ of the crack eigenvalue problem.

Assume that we divide the domain into three subdomains: $\Omega = S_0 \cup S_1 \cup S_2$ as in Fig. 6. Then we may choose the piecewise particular solutions,

$$\begin{cases} v_L = \sum_{i=1}^{L} c_i \dfrac{J_{i-1/2}(kr)}{J_{i-1/2}(kr_0)} \cos\left(i - \frac{1}{2}\right)\theta & \text{in } S_0, \\ v_M = 1 + \sum_{i=1}^{M} a_i \dfrac{J_{2i}(k\rho)}{J_{2i}(k\rho_0)} \sin(2i)\phi & \text{in } S_1, \\ v_N = 1 + \sum_{i=1}^{N} b_i \dfrac{J_{2i}(k\xi)}{J_{2i}(k\xi_0)} \sin(2i)\psi & \text{in } S_2, \end{cases} \tag{5.36}$$

where c_i, a_i and b_i are the unknown coefficients to be sought, and the parameters $r_0 = \rho_0 = \xi_0 = \sqrt{2}/2$. The polar coordinates (r,θ), (ρ,ϕ) and (ξ,ψ) are shown in Fig. 6. Hence there exist the relations of coefficients as in (5.27) and

$$\hat{a}_i = \frac{a_i}{J_{2i-1}(k\rho_0)}, \quad \hat{b}_i = \frac{b_i}{J_{2i-1}(k\xi_0)}. \tag{5.37}$$

---

[3] The minimal eigenvalue is invariant for Ω with a shift $y \to y \pm \frac{1}{2}$.

Table 5
The minimal and the next minimal eigenvalues from the TM for the crack problem

L	$\sqrt{\tilde{\lambda}_{\min}}$	$\lambda_{\min}(\mathbf{A})$	$\sqrt{\dfrac{\lambda_{\min}(\mathbf{A})}{\lambda_{\text{next}}(\mathbf{A})}}$	$\\|E\\|_B$
8	2.8933 4100 66	0.148 (−4)	0.343 (−2)	1.07
12	2.8933 2486 97	0.192 (−7)	1.02 (−3)	1.06
16	2.8933 2486 56	0.699 (−10)	0.750 (−5)	1.04
20	2.8933 2524 69	0.572 (−12)	0.679 (−6)	0.647
L	$\sqrt{\tilde{\lambda}_{\text{next}}}$	$\lambda_{\min}(\mathbf{A})$	$\sqrt{\frac{\lambda_{\min}(\mathbf{A})}{\lambda_{\text{next}}(\mathbf{A})}}$	$\\|E\\|_B$
8	4.0797 8981 09	0.714 (−4)	0.672 (−2)	1.15
12	4.0798 6470 52	0.213 (−7)	0.118 (−3)	1.11
16	4.0798 6383 77	0.312 (−10)	0.455 (−5)	0.109
20	4.0798 6425 24	0.108 (−12)	0.269 (−6)	0.250

Table 6
The minimal and the next minimal eigenvalues from the TM for the crack problem by subdomains

L	M	N	$\sqrt{\tilde{\lambda}_{\min}}$	$\lambda_{min}(\mathbf{A})$	$\sqrt{\frac{\lambda_{\min}(\mathbf{A})}{\lambda_{\text{next}}(\mathbf{A})}}$	$\\|E\\|_B$
8	4	4	2.8932 7155 79	0.767 (−6)	0.297 (−2)	1.28
12	6	6	2.8933 2561 34	0.222 (−8)	0.239 (−3)	1.19
16	8	8	2.8933 2545 50	0.109 (−10)	0.223 (−4)	1.14
20	10	10	2.8933 3949 07	0.297 (−12)	0.459 (−5)	0.921
L	M	N	$\sqrt{\tilde{\lambda}_{\text{next}}}$	$\lambda_{\min}(\mathbf{A})$	$\sqrt{\frac{\lambda_{\min}(\mathbf{A})}{\lambda_{\text{next}}(\mathbf{A})}}$	$\\|E\\|_B$
8	4	4	4.0798 6447 00	0.311 (−6)	0.127 (−2)	0.430
12	6	6	4.0798 6371 57	0.248 (−9)	0.521 (−4)	0.403
16	8	8	4.0798 6471 24	0.437 (−12)	0.228 (−5)	0.391
20	10	10	4.0798 6474 89	0.424 (−11)	0.112 (−4)	0.419 (−1)

The computed results are listed in Tables 5 and 6, and the coefficients of the eigenfunction of $\lambda_{\min}$ in Table 7. It can be seen from Tables 5 and 6 that

$$\sqrt{\tilde{\lambda}_{\min}} = 2.893325, \quad \sqrt{\tilde{\lambda}_{\text{next}}} = 4.079864. \tag{5.38}$$

By Mathematica [25], the more accurate eigenvalues of $\lambda_{\min}$ and λ_{next} with 11 significant digits have been obtained as

$$\sqrt{\lambda_{\min}} = 2.8933250269, \quad \sqrt{\lambda_{\text{next}}} = 4.0798641275. \tag{5.39}$$

Compared with (5.39), the values of $\sqrt{\lambda_{\min}}$ and $\sqrt{\lambda_{\text{next}}}$ in (5.38) have six significant digits.

From Table 7 we can see the ratios $\hat{c}_i/\hat{c}_1$ of leading coefficients for $u_1(x, y)$ of $\lambda_{\min}$ to be[4]

$$\frac{\hat{c}_2}{\hat{c}_1} \approx 0, \quad \frac{\hat{c}_3}{\hat{c}_1} \approx 0, \quad \frac{\hat{c}_6}{\hat{c}_1} \approx 0, \quad \frac{\hat{c}_7}{\hat{c}_1} \approx 0, \ldots, \tag{5.40}$$

and ratios $\hat{c}_i/\hat{c}_2$ for $u_2(x, y)$ of λ_{next} to be

$$\frac{\hat{c}_1}{\hat{c}_2} \approx 0, \quad \frac{\hat{c}_4}{\hat{c}_2} \approx 0, \quad \frac{\hat{c}_5}{\hat{c}_2} \approx 0, \quad \frac{\hat{c}_8}{\hat{c}_2} \approx 0, \quad \frac{\hat{c}_9}{\hat{c}_2} \approx 0, \ldots . \tag{5.41}$$

[4] For other symmetric and anti-symmetric eigenfunctions, the similar results as in (5.40) and (5.41) have also been observed.

Table 7
The coefficients of the eigenfunctions for the (a) minimal eigenvalues and (b) the next minimal eigenvalues for the crack problem by the Trefftz method as $L=20$

i	α_i	c_i	$\frac{c_i}{c_1}$	Ratios $\left(\frac{\hat{c}_i}{\hat{c}_1}\right)$
(a)				
1	0.5	0.53254711543759 (6)	0.1000 (1)	0.10000000000000 (1)
2	1.5	−0.93309909466216	−0.1752 (−5)	−0.40838368080115 (−6)
3	2.5	0.14503983732722	0.2724 (−6)	0.78973941708087 (−7)
4	3.5	−0.28545700655157 (6)	−0.5360	−0.32112892008726
5	4.5	−0.25920546902761 (6)	−0.4867	−0.82533962645231
6	5.5	0.57717136438322 (−2)	0.1084 (−7)	0.65589290617239 (−7)
7	6.5	0.10174443125042	0.1911 (−6)	0.49641891637856 (−5)
8	7.5	0.12383285923908 (5)	0.2325 (−1)	0.30267029834767 (1)
9	8.5	−0.46085824093272 (3)	−0.8654 (−3)	−0.64431242483669
10	9.5	−0.67513842437962 (−1)	−0.1268 (−6)	−0.60660068424728 (-3)
11	10.5	0.41876616110534 (−1)	0.7863 (−7)	0.26828471564346 (−2)
12	11.5	0.18287860946787 (3)	0.3434 (−3)	0.91762896898128 (2)
13	12.5	0.37376296841277 (1)	0.7018 (−5)	0.16001621016243 (2)
14	13.5	−0.23556093109558 (−1)	−0.4423 (−7)	−0.93094675577475
15	14.5	0.12483799246683 (−1)	0.2344 (−7)	0.48986024128118 (1)
16	15.5	0.57427287425920 (1)	0.1078 (−4)	0.23944918535756 (5)
17	16.5	−0.12710610870740 (−1)	−0.2387 (−7)	−0.60006496729259 (3)
18	17.5	−0.46219913184119 (−2)	−0.8679 (−8)	−0.26223984979939 (4)
19	18.5	0.66569590965778 (−3)	0.1250 (−8)	0.48018626770272(4)
20	19.5	0.17184551556236	0.3227 (−6)	0.16620681834440 (8)
(b)				
1	0.5	0.75428464744275	0.5382 (−6)	−0.26258647082581 (−6)
2	1.5	0.14014519782431 (7)	0.1000 (1)	0.10000000000000 (1)
3	2.5	−0.95629818186976 (6)	−0.6824	−0.24501413140731
4	3.5	−0.24469604128049	−0.1746 (−6)	−0.72355984687393 (−7)
5	4.5	0.18015630187574	0.1285 (−6)	0.94852597972361 (−7)
6	5.5	−0.61459443064148 (6)	−0.4385	−0.76063624981246
7	6.5	0.17275349424434 (6)	0.1233	0.61879793889902
8	7.5	−0.44716320823631 (−1)	−0.3191 (−7)	−0.54826073662432 (−6)
9	8.5	0.69793691093254 (−1)	0.4980 (−7)	0.33736062432178 (−5)
10	9.5	−0.12196039389009 (4)	−0.8702 (−3)	−0.26266468711605
11	10.5	−0.20639454965325 (4)	−0.1473 (−2)	−0.22067301704717 (1)
12	11.5	−0.47009665845852 (−1)	−0.3354 (−7)	−0.27493354260175 (−3)
13	12.5	0.21119274287301 (−1)	0.1507 (−7)	0.73777983835726(−3)
14	13.5	−0.97400815111797 (1)	−0.6950 (−5)	−0.22030049384368 (1)
15	14.5	−0.19073976558829 (2)	−0.1361 (−4)	−0.30087932757286 (2)
16	15.5	−0.15534114323710 (−1)	−0.1108 (−7)	−0.18311443354442
17	16.5	0.23687602954159 (−2)	0.1690 (−8)	0.22255500341053
18	17.5	−0.52779222782251 (−1)	−0.3766 (−7)	−0.41987157072731 (2)
19	18.5	−0.37373242631831	−0.2667 (−6)	−0.26648799185682 (4)
20	19.5	−0.23629938531931 (−2)	−0.1686 (−8)	−0.15937118358056 (3)

By Mathematica [25] using more significant digits, we obtain more accurate ratios. For $u_1(x,y)$ of $\lambda_{\min}$, the ratios $\hat{c}_i/\hat{c}_1$ are given as

$$\frac{\hat{c}_2}{\hat{c}_1}=-0.2813(-19),\quad \frac{\hat{c}_3}{\hat{c}_1}=0.2491(-19),\quad \frac{\hat{c}_4}{\hat{c}_1}=-0.3211285648,$$
$$\frac{\hat{c}_5}{\hat{c}_1}=-0.8253397549,\quad \frac{\hat{c}_6}{\hat{c}_1}=0.8183(-19),\quad \frac{\hat{c}_7}{\hat{c}_1}=-0.1656(-18), \tag{5.42}$$

and those for $u_2(x, y)$ of λ_{next} as

$$\frac{\hat{c}_1}{\hat{c}_2} = -0.4585(-19), \quad \frac{\hat{c}_3}{\hat{c}_2} = -0.2450141227, \quad \frac{\hat{c}_4}{\hat{c}_2} = -0.4585(-19), \quad \frac{\hat{c}_5}{\hat{c}_2} = -0.3344(-19),$$
$$\frac{\hat{c}_6}{\hat{c}_2} = -0.7606363529, \quad \frac{\hat{c}_7}{\hat{c}_2} = 0.6187975895, \quad \frac{\hat{c}_8}{\hat{c}_2} = -0.4904(-19). \tag{5.43}$$

From (5.42) and (5.43), Eqs. (5.40) and (5.41) are again confirmed. Hence we may simply assume the following trivial coefficients:

$$\hat{c}_{4i-2} = \hat{c}_{4i-1} = 0, \quad i = 1, 2, \ldots \quad \text{for } u_1(x, y),$$
$$\hat{c}_{4i-3} = \hat{c}_{4i} = 0, \quad i = 1, 2, \ldots \quad \text{for } u_2(x, y). \tag{5.44}$$

Then the admissible functions (5.26) and v_L in (5.36) can be simplified by

$$v^+ = \sum_{i=1}^{L} \left\{ c^*_{2i-1} \frac{J_{4i-7/2}(kr)}{J_{4i-7/2}(kr_0)} \cos\left(4i - \frac{7}{2}\right)\theta + c^*_{2i} \frac{J_{4i-1/2}(kr)}{J_{4i-1/2}(kr_0)} \cos\left(4i - \frac{1}{2}\right)\theta \right\} \tag{5.45}$$

for $u_1(x, y)$, and

$$v^+ = \sum_{i=1}^{L} \left\{ c^*_{2i-1} \frac{J_{4i-5/2}(kr)}{J_{4i-5/2}(kr_0)} \cos\left(4i - \frac{5}{2}\right)\theta + c^*_{2i} \frac{J_{4i-3/2}(kr)}{J_{4i-3/2}(kr_0)} \cos\left(4i - \frac{3}{2}\right)\theta \right\} \tag{5.46}$$

for $u_2(x, y)$, where L is even, and the coefficients c_i^* with star are used to distinguish c_i in (5.26). By using the simplified particular solutions (5.45) and (5.46), the numerical solutions by the TM are very close to those by using (5.26). We omit the detailed numerical results, but only list in Table 8

the approximate coefficients in (5.36), where v_L is replaced by (5.45) and (5.46) for $u_1(x, y)$ and $u_2(x, y)$, respectively.

Remark 5.1. Let us provide a physical meaning for the eigenvalue problems in (5.1) and (5.23). In Courant and Hilbert [6, p. 297], The basic model (5.1) results from the vibrating homogeneous membrane with the fixed displacements on the exterior boundary Γ of Ω. The $\sqrt{\lambda}$ and the u are the frequency and the amplitude of vibrating waves, respectively. The membrane vibration with the minimal frequency (i.e., the eigenpair of the minimal eigenvalue $\lambda_{\min}$ and its corresponding eigenfunction) is most interesting in both theory and application, see [6]. Next, let us consider a rectangular membrane with an inside crack $\overline{OD}$ (see Fig. 7), where the displacements on $\Gamma \cup \overline{OD}$ are fixed during the vibrating. The crack eigenvalue problem (5.23) results from a symmetry of the vibrating membrane shown in Fig. 7. For the crack equilibrium problem, there exist numerous reports of numerical methods and numerical results. However, for the crack eigenvalue problems, this paper is the first time to provide the numerical solutions by the TM. Since the solutions with the coefficients in Tables 7 and 8 by the TM are highly accurate, they can be used as the *true* solutions to test other numerical methods for eigenvalue problems with singularity.

6. Summaries and discussions

To close this paper, let us make a few remarks.

(1) The numerical algorithms rely on the Helmholtz equation (2.5) by modifying k to lead to a degeneracy. The degeneracy is measured by the infinitesimal values of the minimal eigenvalue $\lambda_{\min}(\mathbf{A})$ of the stiffness matrix $\mathbf{A}(k)$ in (2.14), and the modification to k is realized by the iterative algorithms in Section 2.2, based on the fact that the eigenfunctions of (2.4) will dominate the solutions of (2.5) when a degeneracy occurs.
(2) The main results of error analysis are given in Theorems 3.1, 4.1 and 4.2, as well as Corollary 3.1, which indicate that the errors of the solutions of the leading eigenvalues and their eigenfunctions can be measured by $\sqrt{\lambda_{\min}(\mathbf{A})}$. Such conclusions have been confirmed by the numerical experiments in Section 5.

Table 8
The coefficients of the eigenfunctions for the (a) minimal eigenvalues and (b) the next minimal eigenvalues for the crack problem with the shortlist coefficients by the Trefftz method as $L = 20$ and $N = M = 10$ in subdomains

c_i^*	α_i	c_i^*	$\frac{c_i^*}{c_1^*}$	Ratios $\left(\frac{\hat{c}_i^*}{\hat{c}_1^*}\right)$
(a)				
c_1^*	0.5	−0.30778385362611 (7)	0.1000 (1)	0.10000000000000 (1)
c_2^*	3.5	0.14621985564119 (6)	−0.4751 (−1)	−0.32112683765581
c_3^*	4.5	0.89321048082330 (5)	−0.2902 (−1)	−0.82533661779926
c_4^*	7.5	−0.14014784360115 (4)	0.4553 (−3)	0.30267798094757 (1)
c_5^*	8.5	0.36363026198509 (2)	−0.1181 (−4)	−0.64401388090113
c_6^*	11.5	−0.49768655603368 (1)	0.1617 (−5)	0.91965094670667 (2)
c_7^*	12.5	−0.81653033273586 (−1)	0.2653 (−7)	0.18322339576440 (2)
c_8^*	15.5	−0.28574875276399 (−1)	0.9284 (−8)	0.17918763946890 (5)
c_9^*	16.5	0.20203718849703 (−2)	−0.6564 (−9)	−0.20361260416549 (5)
c_{10}^*	19.5	−0.29989648939942 (−2)	0.9744 (−9)	0.17669152572679 (9)
a_i	i	a_i	$\frac{a_i}{a_1}$	Ratios $\left(\frac{\hat{a}_i}{\hat{a}_1}\right)$
a_1	2	−0.30870864864183 (7)	0.1000 (1)	0.10000000000000 (1)
a_2	4	0.13267913489024 (6)	−0.4298 (−1)	−0.42314432754102
a_3	6	−0.24137383758068 (5)	0.7819 (−2)	0.20739216504490 (1)
a_4	8	−0.14491091653193 (4)	0.4694 (−3)	0.64407532955675 (1)
a_5	10	0.51100994160756 (3)	−0.1655 (−3)	−0.19120060568909 (3)
a_6	12	0.36632601757803 (2)	−0.1187 (−4)	−0.17036350792643 (4)
a_7	14	−0.16232840981491 (2)	0.5258 (−5)	0.12988947718730 (6)
a_8	16	−0.13347398477504 (1)	0.4324 (−6)	0.24293918124378 (7)
a_9	18	0.52849875158320	−0.1712 (−6)	−0.27946963324189 (9)
a_{10}	20	0.48334466869797 (−1)	−0.1566 (−7)	−0.92329368183736 (10)
b_i	i	b_i	$\frac{b_i}{b_1}$	Ratios $\left(\frac{\hat{b}_i}{\hat{b}_1}\right)$
b_1	2	−0.12787126642683 (7)	0.1000 (1)	0.10000000000000 (1)
b_2	4	−0.32031576689594 (6)	0.2505	0.24662666991583 (1)
b_3	6	−0.99979969522290 (4)	0.7819 (−2)	0.20739151318936 (1)
b_4	8	0.34984590002732 (4)	−0.2736 (−2)	−0.37539473736210 (2)
b_5	10	0.21165845388863 (3)	−0.1655 (−3)	−0.19119272540117 (3)
b_6	12	−0.88438923988631 (2)	0.6916 (−4)	0.99295162194911 (4)
b_7	14	−0.67153595351149 (1)	0.5252 (−5)	0.12972525531485 (6)
b_8	16	0.32223470427494 (1)	−0.2520 (−5)	−0.14159537860692 (8)
b_9	18	0.21674276928799	−0.1695 (−6)	−0.27670124131640 (9)
b_{10}	20	−0.11668972546849	0.9126 (−7)	0.53813517357257 (11)
(b)				
c_i^*	α_i	c_i^*	$\frac{c_i^*}{c_1^*}$	Ratios $\left(\frac{\hat{c}_i^*}{\hat{c}_1^*}\right)$
c_1^*	1.5	0.61599463304656 (8)	0.1000 (1)	0.10000000000000 (1)
c_2^*	2.5	−0.12063691541673 (8)	−0.1958	−0.24501413291495
c_3^*	5.5	−0.17750818372509 (7)	−0.2882 (−1)	−0.76063638180196
c_4^*	6.5	0.33526817833132 (6)	0.5443 (−2)	0.61879767433502
c_5^*	9.5	−0.76567762005311 (3)	−0.1243 (−4)	−0.26265829416980
c_6^*	10.5	−0.89950924012844 (3)	−0.1460 (−4)	−0.22068737654207 (1)
c_7^*	13.5	−0.14773427746429 (1)	−0.2398 (−7)	−0.22560483930827 (1)
c_8^*	14.5	−0.19481134770270 (1)	−0.3163 (−7)	−0.29626194827807 (2)
c_9^*	17.5	0.14212054712923 (−3)	0.2307 (−11)	0.31529612445227 (1)
c_{10}^*	18.5	−0.26136744437305 (−1)	−0.4243 (−9)	−0.73936509686488 (4)

Table 8 *(Continued)*

a_i	i	a_i	$\frac{a_i}{a_1}$	Ratios $\left(\frac{\hat{a}_i}{\hat{a}_1}\right)$
a_1	2	−0.28642405118339 (8)	0.1000 (1)	0.10000000000000 (1)
a_2	4	−0.16281863883837 (8)	−0.5685	−0.23420622751470 (1)
a_3	6	−0.35191501695889 (6)	−0.1229 (−1)	−0.64166218136308
a_4	8	−0.77722517142999 (5)	−0.2714 (−2)	−0.35595897889798 (1)
a_5	10	0.29439863060583 (4)	0.1028 (−3)	0.55852293694566 (1)
a_6	12	0.10051318255285 (4)	0.3509 (−4)	0.11743714949760 (3)
a_7	14	−0.49125947629686 (2)	−0.1715(−5)	−0.49131093584465 (3)
a_8	16	−0.21315366087734 (2)	−0.7442 (−6)	−0.24186842518176 (5)
a_9	18	0.11566375414079 (1)	0.4038 (−7)	0.19052735996715 (6)
a_{10}	20	0.57289419741525	0.2000 (−7)	0.17055073440733 (8)
b_i	i	b_i	$\frac{b_i}{b_1}$	Ratios $\left(\frac{\hat{b}_i}{\hat{b}_1}\right)$
b_1	2	−0.69148885713114 (8)	0.1000 (1)	0.10000000000000 (1)
b_2	4	−0.67441688413979 (7)	0.9753 (−1)	0.40183434219792
b_3	6	0.84959770616639 (6)	−0.1229 (−1)	−0.64166192820582
b_4	8	−0.32193720702407 (5)	0.4656 (−3)	0.61072902993556
b_5	10	−0.71073636012472 (4)	0.1028 (−3)	0.55851913698850 (1)
b_6	12	0.41633923410504 (3)	−0.6021 (−5)	−0.20149028579870 (2)
b_7	14	0.11855106927365 (3)	−0.1714 (−5)	−0.49110602534763 (3)
b_8	16	−0.88291137184113 (1)	0.1277 (−6)	0.41498059440972 (4)
b_9	18	−0.27796176603088 (1)	0.4020 (−7)	0.18965723937764 (6)
b_{10}	20	0.23730054594633	−0.3432 (−8)	−0.29261878633888 (7)

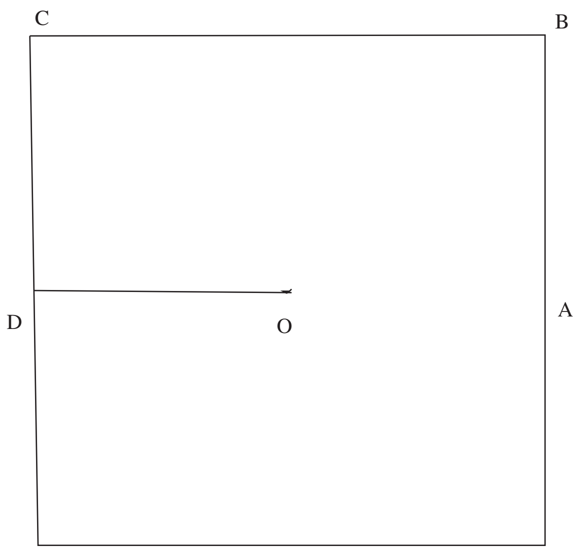

Fig. 7. A rectangular membrane with an inside crack.

(3) A basic model of eigenvalue problems is given in Section 5.1, and the new crack eigenvalue problem with singularity is explored in Section 5.2. Since the eigenvalues and the expansion coefficients of eigenfunctions are very accurate, they can be regarded as the *exact* solutions, which may provide an evaluation of the true errors of solutions by other numerical methods, e.g., FEM, FDM, FVM, BEM, etc.

(4) This paper may be regarded as a further development of Fox et al. [8] by using piecewise particular solutions. The methods in [8] use *uniform* particular solutions to seek the eigenvalues of (2.1). The algorithms in this paper adopt

piecewise particular solutions, which may lead to a wide range of applications of complicated eigenvalue problems, for instance those with multiple singularities (see [12]). In these cases, we may partition the solution domain into finite subdomains, local particular solutions can be employed in the subdomains, to extend the collocation TM for the eigenvalue problems on rather arbitrary domains.

Acknowledgements

I am very grateful to Prof. B. Sommeijer, Dr. H. T. Huang and the referee for their valuable comments and suggestions.

References

[1] M. Abramowitx, I.A. Stegun (Eds.), Handbook of Mathematical Functions, with Formulas, Graphs, and Mathematical Tables, Dover Publications Inc., New York, 1972.
[2] K.E. Atkinson, An Introduction to Numerical Analysis, second ed., Wiley, New York, 1989.
[3] I. Babuska, J. Osborn, Eigenvalue problems, in: P.G. Ciarlet, J.L. Lions (Eds.), Handbook of Numerical Analysis, vol. II, Finite Element Methods (Part I), North-Holland, Amsterdam, 1991, pp. 641–787.
[4] S. Bergman, Integral Operators in the Theory of Linear Partial Differential Equations, Springer, Berlin, New York, 1969.
[5] G. Birkhoff, R.E. Lynch, Numerical Solution of Elliptic Problems, SIAM, Philadelphia, 1984.
[6] R. Courant, D. Hilbert, Methods of Mathematical Physics, vol. I, Wiley, New York, 1953.
[7] S.C. Eisenstat, On the note of convergence of the Bergman–Vekua methods for the numerical solution of elliptic boundary-value problems, SIAM J. Numer. Anal. 11 (1974) 654–680.
[8] L. Fox, P. Henrici, C. Molor, Approximations and bounds for eigenvalues of elliptic operators, SIAM J. Numer. Anal. 4 (1967) 89–102.
[9] G.H. Golub, C.F. van Loan, Matrix Computation, second ed., The John Hopkins University Press, Baltimore, 1989.
[10] C.A. Hall, T.A. Porsching, Numerical Analysis of Partial Differential Equations, Prentice-Hall, Englewood cliffs, NJ, 1990.
[11] J.R. Kuttler, V.G. Sigilloto, Eigenvalues of the Laplacian in two dimensions, SIAM Rev. 26 (1984) 163–193.
[12] Z.C. Li, Combined Methods for Elliptic Equations with Singularities, Interfaces and Infinities, Kluwer Academic Publishers, Dordrecht, 1998.
[13] Z.C. Li, The Trefftz method for the Helmholtz equation with degeneracy, Technical Report, Department of Applied Mathematics, National Sun Yat-sen University, Taiwan, 2004.
[14] Z.C. Li, T.T. Lu, H.S. Tsai, A.H.D. Cheng, The Trefftz methods for solving eigenvalues problems, Engrg. Anal. Boundary Elements, to appear.
[15] Z.C. Li, R. Mathon, The Trefftz method for solving elliptic problems on unbounded domains, J. Comput. Phys. 89 (1990) 414–431.
[16] Z.C. Li, R. Mathon, Error and stability analysis of boundary methods for elliptic problems with interfaces, Math. Comp. 54 (1990) 41–61.
[17] Z.C. Li, R. Mathon, P. Sermer, Boundary methods for solving elliptic problems with singularities and interfaces, SIAM J. Numer. Anal. 24 (1987) 487–498.
[18] R. Mathon, P. Sermer, Numerical solution of the Helmholtz equation, Congr. Numer. 34 (1982) 313–330.
[19] M. Ortega, Numerical Analysis, A Second Course, SIAM, Philadelphia, 1990.
[20] B.N. Parlett, The Symmetric Eigenvalue Problems, Prentice-Hall, Englewood Cliffs, NJ, 1980.
[21] G. Strang, G.J. Fix, An Analysis of Finite Element Methods, Prentice-Hall, Englewood Cliffs, NJ, 1973.
[22] E. Trefftz, Ein Gegenstuck zum Ritz'schen Verfahren, Proceedings of the 2nd Ind Congr Appl. Mech., Zurich, 1926, pp. 131–137.
[23] I.N. Vekua, New Method for Solving Elliptic Equations, North-Holland, Amsterdam, New York, 1967.
[24] J.H. Wilkinson, The Algebraic Eigenvalue Problems, Oxford University Press, Oxford, 1965.
[25] S. Wolfram, Mathematica, A System for Doing Mathematics by Computer, second ed., Addison-Wesley Publishing Company, New York, 1991.